Collapse transition and crossover scaling for self-avoiding walks on the diamond lattice

1982 J. Phys. A: Math. Gen. 15 2879

(http://iopscience.iop.org/0305-4470/15/9/036)

J. Phys. A: Math. Gen. **15** (1981) 2879–2897. Printed in Great Britain

Collapse transition and crossover scaling for self-avoiding walks on the diamond lattice

K Kremer, A Baumgärtner† and K Binder

Institut für Festkörperforschung der Kernforschungsanlage Jülich, Postfach 1913, D-5170 Jülich, Federal Republic of Germany

Received 10 March 1982

Abstract. A Monte Carlo study of self-avoiding walks on the diamond lattice is presented. This model incorporates some of the steric effects and short-range stiffness of real alkanes, and for a nearest-neighbour attractive interaction $-\varepsilon$ is found to have a collapse transition at $k_B\theta/\varepsilon = 2.25 \pm 0.05$. The behaviour of the chains in the vicinity of this θ-temperature is analysed with the help of recent 'crossover scaling' theories. It is shown that for finite chain length N there is a rather broad θ-region where the chains' behaviour is quasi-ideal. The width of this region w_θ behaves as $w_\theta \propto N^{-1/2}$, consistent with the blob picture. The peak of the specific heat occurs at the boundary between the θ-region and the region of collapsed chains. We also give rough estimates for the scaling functions describing the crossovers of the end-to-end distance and structure factor of the chains.

1. Introduction

There has been great interest in the statistics of polymer chains in the presence of intramolecular forces (see e.g. the review by de Gennes (1979)). The intermolecular forces consist of a (hard core) repulsion of the monomers of the chain at short distances, and an attractive interaction of longer range. At the θ-temperature both contributions effectively cancel each other, and the chains behave essentially as ideal random walks (Flory 1967, 1969). Below this temperature the chain collapses in a condensed state. Although there is some experimental evidence for this behaviour (Cuniberti and Bianchi 1974, Mazur and McIntyre 1975, Nierlich *et al* 1978, Swislov *et al* 1980, Perzynski *et al* 1982), it is rather difficult to obtain complete and fully conclusive results because one is restricted to solutions of extremely dilute polymer concentration. Thus many predictions of the numerous analytical theories (Edwards 1965, 1970, Domb 1974, Lifshitz *et al* 1978, de Gennes 1972, 1975, 1977, 1978, Moore 1977, Daoud and Jannink 1976, Duplantier 1980) are as yet untested.

Thus computer experiments should be an important check of the theory. Numerous Monte Carlo studies of corresponding polymer models have already been performed, both on lattices (Mazur and McCrackin 1968, McCrackin *et al* 1973, Finsy *et al* 1975, Janssens and Bellemans 1976, Lal and Spencer 1971, Clark and Lal 1977), for which exact enumerations were also performed (Fisher and Hiley 1961, Rapaport 1974, 1977), and also in the continuum (Baumgärtner 1980, Webman *et al* 1981).

† Address during 1982: IBM Research Laboratory, 5600 Cottle Road, San José, CA 95193, USA.

0305-4470/82/092879+19$02.00

But a detailed numerical analysis of the crossover of the various quantities as one passes the θ-region, in the light of the theories mentioned above, has not yet been performed. This is the aim of the present paper.

Of course, the analytical theories concern the asymptotic properties of very long chains ($N \to \infty$), while numerical studies are performed for rather small N. Hence these asymptotic properties are only accessible from extrapolations, which are sometimes uncertain or even impossible. On the other hand, there is interest also in properties of rather short real polymer chains, particularly for alkanes ($CH_3(CH_2)_nCH_3$, with $10 \leqslant n \leqslant 10^2$). There the angles between subsequent C–C bonds are those of a tetrahedral structure (at room temperature deviations from these angles are less then 3°, see e.g. Lal and Spencer (1971)). Therefore as a model which reproduces some features of these local polymer structures, we consider chains on the diamond lattice, which has such tetrahedral angles. The repulsive part of the interaction is modelled as usual by choosing self-avoiding walks (SAW), the attractive part by a nearest-neighbour energy, $-\varepsilon$. In the following two sections this model is explained in more detail, as well as the various Monte Carlo procedures used. In § 4 the numerical results are presented and compared with recent theoretical and experimental work, while § 5 contains our conclusions.

2. Description of the model

Our model of a polymer consists of N bonds of fixed lengths l, thus connecting $N+1$ monomeric units, on a diamond lattice which has the coordination number $q = 4$. For understanding the Monte Carlo process it is necessary to consider briefly the geometry of this lattice (for more details see Gény and Monnerie (1979), Kremer (1982)). We describe the lattice by two FCC sublattices, their origins being shifted by the vector (1, 1, 1). The unit cell then has the volume $4 \times 4 \times 4$. Each chain is then built up as a sequence of points taken alternately from the two sublattices, figure 1(*a*). The monomers of a chain are hence connected alternatingly by primed or unprimed bond vectors defined by

$$\begin{gathered} a = (1, 1, 1), \qquad b = (1, -1, -1), \qquad c = (-1, 1, -1), \qquad d = (-1, -1, 1), \\ a' = -a, \qquad b' = -b, \qquad c' = -c, \qquad d' = -d. \end{gathered} \tag{1}$$

For numerical calculations it is useful to choose only even numbers of such bonds, each bond of length $l = \sqrt{3}$.

We test our Monte Carlo methods by considering also non-reversal random walks (NRRW) rather than SAWs, since for the NRRW exact calculations exist for arbitrary N (Domb and Fisher 1958). The NRRW, for which direct reversals such as $ca'ab'$ are forbidden, is a random walk with $q = 3$.

In our model with nearest-neighbour interactions, temperature comes into play by the Boltzmann factor $\exp(n_\varepsilon/T)$, where n_ε is the number of nearest-neighbour contacts (omitting the trivial ones along the chain and setting $\varepsilon/k_B \equiv 1$). Of course, this is only a rather qualitative description of the interactions, mediated by the solvent in a real polymer solution (Flory 1967, 1969), but it has the essential feature of competition between short-range repulsion (due to the SAW condition) and longer-range attraction. Apart from ε, there is no energy distinguishing trans and gauche bonds as done e.g. by Lal and Spencer (1971) and Clark and Lal (1977). Hence in

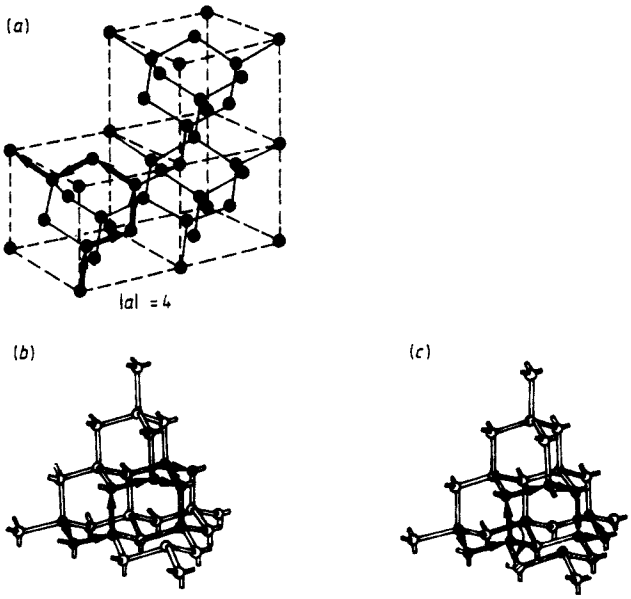

Figure 1. (*a*) Diamond lattice with a chain starting at (0, 0, 0) and ending at (0, 4, 4). (*b*) Three-bond motion of a chain on the diamond lattice. (*c*) Four-bond motion of a chain on the diamond lattice.

our case the steric properties and stiffness of the chains result from the non-uniformity of the lattice together with the SAW condition only.

3. Discussion of the Monte Carlo methods used

Depending on the temperature regime and the chain lengths, we either use simple sampling (SS) or importance sampling (Binder 1979) methods, using either 'reptation' or 'three–four bond motions', for importance sampling.

In the SS method one has to stop the walk and start a completely new chain as soon as the SAW condition is violated, in order to do an unbiased sampling (for more details see Kremer *et al* (1981), Kremer (1982)). Thus one can calculate a broad range of chain lengths N in *one* run. One samples the distribution function $P_N(n_\varepsilon)$ of the number of nearest-neighbour contacts. Temperature-dependent averages are then obtained afterwards by the Boltzmann weighting factors $\exp(n_\varepsilon/T)$. Of course, for low temperatures where the main contribution comes from large n_ε, i.e. the 'wing' of the distribution $P_N(n_\varepsilon)$, the lattice must be sampled extremely accurately to obtain meaningful estimates. Thus, for $N = 100$ up to 2×10^6 configurations were performed. The accuracy is also checked by performing some 'dynamic' importance sampling runs for the same parameters as the SS runs.

Part of our work, using importance sampling, was done using the 'reptation' method (Wall and Mandel 1971; see also Webman *et al* 1980, Kremer *et al* 1981, Kremer 1981). This method turned out to be useful at high temperatures and $N < 100$.

Therefore we introduce another dynamical Monte Carlo method based on internal motions of the chain. A similar approach was taken by Gény and Monnerie (1979)

in their study of relaxations inside NRRWs with certain steric energies, but their method involves a bias. Using their original method therefore yields unsatisfactory results in our case (Kremer 1982). Thus it is necessary to describe our approach in more detail.

One needs to move at least three bonds for simple internal motions. The only possible three-bond motion (figure 1(*b*)) is an interchange of bond vectors,

$$ab'cd'a \rightarrow ad'cb'a. \tag{2}$$

No new bond vector is created in such a motion; new bond vectors can only diffuse into the chain from 'freely rotating' endbonds, where this conservation law is violated. Also the chain length N must be even: otherwise both endbonds would belong to the same set (e.g. the unprimed one), and rotating ends could only create new bonds in this set. It turns out that also for N even this diffusion of bond vectors is very slow, since SAW conditions must be obeyed; thus three-bond motion alone would be insufficient to reach thermal equilibrium during reasonable simulation times. Therefore other motions involving more bonds must also be included. The only four-bond motion which cannot be built up by a sequence of three-bond motions is (Gény and Monnerie 1979) of the type

$$b'ab'ca'c \rightarrow b'db'cd'c. \tag{3}$$

This motion (figure 1(*c*)) creates two new bond vectors inside the chain. One can show (Kremer 1982) that this four-bond rotation can never intersect with any other bonds of the same chain (or other chains, respectively) at the lattice, if the SAW condition is fulfilled. Contrary to chains in the continuum (Baumgärtner 1981), possible effects due to chain entanglement are hence automatically taken into account, and need not be added by an extra restriction as in the continuum case. Since there are two inner bonds in the sequence equation (3), two kinds of four-bond motion exist. We then combine the three types of motion as follows. First, by a random number a bond is selected. If it is an outer bond, a random number is chosen to decide to which of the three other possible orientations on the lattice it is attempted to rotate. If it is an inner bond, a random number is chosen to select randomly one of the three types of motion. Then one asks for the steric or SAW possibility of the desired motion.

For NRRWs it is easy to show that the condition of detailed balance is then obeyed (Kremer 1982). Since for chains of up to five bonds the SAW condition is then automatically fulfilled, detailed balance is fulfilled for SAWs also. We have then checked our programs by computing the end-to-end distance

$$R_N^2 = \langle (\boldsymbol{r}_1 - \boldsymbol{r}_{N+1})^2 \rangle, \tag{4}$$

where $\boldsymbol{r}_i$ labels the position of the ith monomer along the chain, and by comparing it with exactly known results for $\varepsilon = 0$. For NRRWs, an exact formula of Domb and Fisher (1958) is available for arbitrary N, while for SAWs, exact countings of Wall and Hioe (1970) extend up to $N = 20$. We get excellent agreement with these results. Defining one time-step of the simulation as N attempted motions, we define the autocorrelation function of $\langle R_N^2 \rangle$ as

$$A_N(t) = [\langle R_N^2(t_0) R_N^2(t_0 + t) \rangle - \langle R_N^2 \rangle^2] / (\langle R_N^4 \rangle - \langle R_N^2 \rangle^2), \tag{5}$$

which yields the relaxation time τ_N,

$$\tau_N = \int_0^\infty A_N(t)\,\mathrm{d}t. \tag{6}$$

As desired, Rouse dynamics applies for the chosen motions, i.e. (see Verdier 1966, Hilhorst and Deutch 1975, Lax and Brender 1977)

$$\tau_N \propto N^2. \tag{7}$$

With this method, chains are simulated up to $N = 200$ for temperatures between $T = \infty$ (i.e. ordinary SAWs) and $T = 1$ ($\varepsilon/k_B \equiv 1$). Configurations were stored after each $(1-5)N^2$ steps, the precise number depending on the acceptance rate of the motions, in order to have statistically independent observations (Binder 1979), and then averages of all desired quantities taken. The random number generator R250 of Kirkpatrick and Stoll (1981) was used throughout.

4. Numerical results and their theoretical interpretation

4.1. End-to-end distance, gyration radius, density and structure factor

We are most interested in the region around the θ-temperature here. There the chains should show a quasi-ideal behaviour due to an effective cancellation of the repulsive and attractive parts of the interaction. The first definition of the θ-temperature considers the expansion of the free energy in terms of the density, and defines θ as the 'Boyle temperature' where the second virial coefficient vanishes (Flory 1967, Moore 1977, de Gennes 1975). In the second definition, one requires that both $\langle R_N^2 \rangle$ and the radius of gyration

$$\langle R_G^2 \rangle = \frac{1}{(N+1)^2} \left\langle \sum_{i=1}^{N} \sum_{j=i+1}^{N+1} (\boldsymbol{r}_i - \boldsymbol{r}_j)^2 \right\rangle \tag{8}$$

behave asymptotically as a random coil. Since the θ-point can be interpreted as a tricritical point (de Gennes 1977, 1978),

$$\langle R_N^2 \rangle \propto \langle R_G^2 \rangle \propto N^{2\nu_t}, \qquad \nu_t = \tfrac{1}{2}, \qquad N \to \infty, \qquad T = \theta. \tag{9}$$

For $T > \theta$, the chain should still exhibit SAW behaviour, while for $T < \theta$ it collapses to a condensed state,

$$\langle R_N^2 \rangle \propto \langle R_G^2 \rangle \propto N^{2\nu}, \qquad \begin{matrix} \nu \approx 0.59, & T > \theta, \\ \nu = \tfrac{1}{3}, & T < \theta, \end{matrix} \qquad N \to \infty. \tag{10}$$

Of course, these laws hold asymptotically for $N \to \infty$. For finite N, there occurs a smooth crossover between these various laws, and the quasi-ideal behaviour of equation (9) is seen in a region of temperatures around $T = \theta$; the width of this region depends on N.

This behaviour is established rather clearly from our numerical data (figure 2). The flat regions of $\langle R_N^2 \rangle / l^2 N$ and $\langle R_G^2 \rangle / l^2 N$ define the θ region, and extrapolating towards $N \to \infty$ we estimate from figure 2

$$\theta = 2.25 \pm 0.10. \tag{11}$$

Similar to other results for chains on lattices (Curro and Schäfer 1980, Clark and Lal

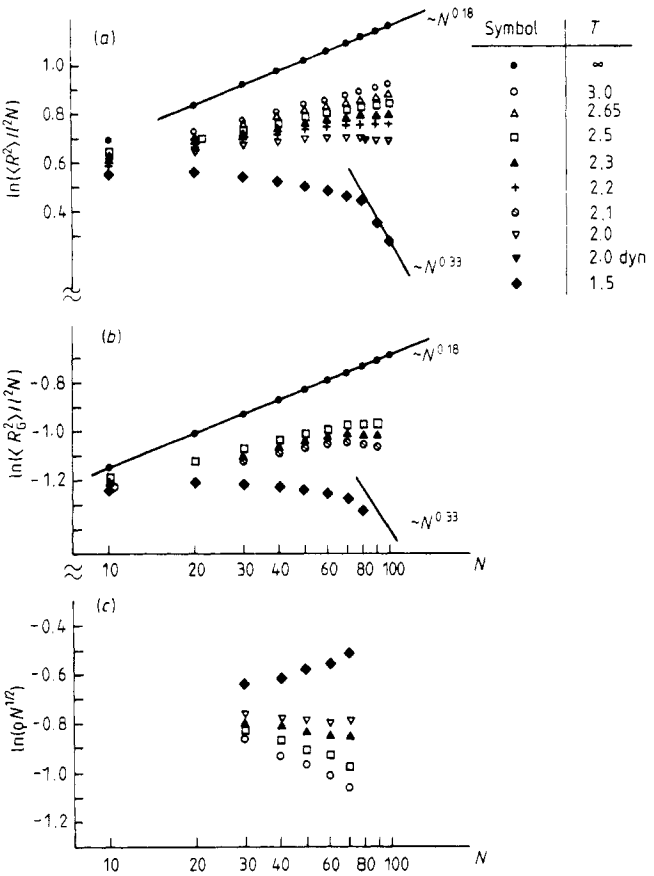

Figure 2. Log–log plots of (*a*) $\langle R_N^2\rangle/l^2N$, (*b*) $\langle R_G^2\rangle/l^2N$ and (*c*) normalised density $\rho N^{1/2}$ against N. Data are obtained by SS methods, with still 10^6 realisations for $N = 100$; at $N = 80$, $T = 2$ a result of dynamical three–four bond motions, where 2×10^4 observations were averaged, is included. The straight line fitting the data at $T = \infty$ has the slope expected from $\nu = 0.59$.

1977), short chains always have a tendency to be SAWs even for $T < \theta$. This is a sort of 'chain stiffness' induced by the short-range NRRW condition. We also calculate the density ρ,

$$\rho = N/\langle R_G^3\rangle. \tag{12}$$

Similar to the behaviour of $\langle R_G^2\rangle/N$, the quantity $\rho N^{1/2}$ becomes flat inside the θ-region. While for $T < \theta$ one expects $\rho(N \to \infty) \to$ constant, one still finds pronounced N-dependence of ρ down to $T \approx 1.5$ for the chain lengths studied, and also the asymptotic laws, equation (10), are not yet valid. This implies that the crossover region is rather broad. These results are qualitatively similar to previous work on chains in the continuum (Baumgärtner 1980), but there a detailed study of the θ-region has not been performed.

We also obtain the structure factor

$$S(\boldsymbol{k}) = \left\langle \frac{1}{(N+1)^2} \left| \sum_{j=1}^{N+1} \exp(i\boldsymbol{k} \cdot \boldsymbol{r}_j) \right|^2 \right\rangle, \tag{13a}$$

in its spherical average

$$S(k)=\left\langle \frac{1}{(N+1)^2}\left\{\left|\sum_{j=1}^{N+1}\exp(i\boldsymbol{k}\cdot\boldsymbol{r}_j)\right|^2\right\}_{|\boldsymbol{k}|}\right\rangle. \tag{13b}$$

In the spherical average, we get rid of the effects due to the orientation of lattice axes, which are artificial if one wishes to consider an ensemble of chains in a dilute solution, where no preferred axes exist. According to Debye (1947) and Farnoux *et al* (1978), we have

$$S(k)\propto k^{-1/\nu}/N, \qquad (2\pi)^2/\langle R_N^2\rangle \ll k^2 \ll (2\pi)^2/l^2, \tag{14a}$$

$$S(k)\approx 1/N, \qquad (2\pi)^2/l^2 \ll k^2. \tag{14b}$$

Excellent agreement with equation (14) is noted at infinite temperature (figure 3). In the θ-region $\nu_t=\frac{1}{2}$, therefore $k^2S(k)$ should approach a constant in the region where equation (14*a*) is valid. Figure 4 shows that only for $T\approx 2.3$ is there an appreciable region of k where $k^2S(k)$ is constant, and hence $\theta\approx 2.3$, consistent with equation (11). Varying N at fixed T, one expects that $S(k)$ is a function of the scaled variable $q=kN^{\nu}$ only (see e.g. Baumgärtner and Binder 1979). This type of scaling is verified for two temperatures in figure 5. The desired slope (q^{-2}) is seen clearly for temperatures throughout the θ-region.

4.2. Crossover scaling analysis

We now consider the scaling of $\langle R_N^2\rangle$ and $S(k)$ as the temperature distance $\tau=|(T-\theta)/\theta|$ from the θ-temperature is varied, to study the theoretical predictions of

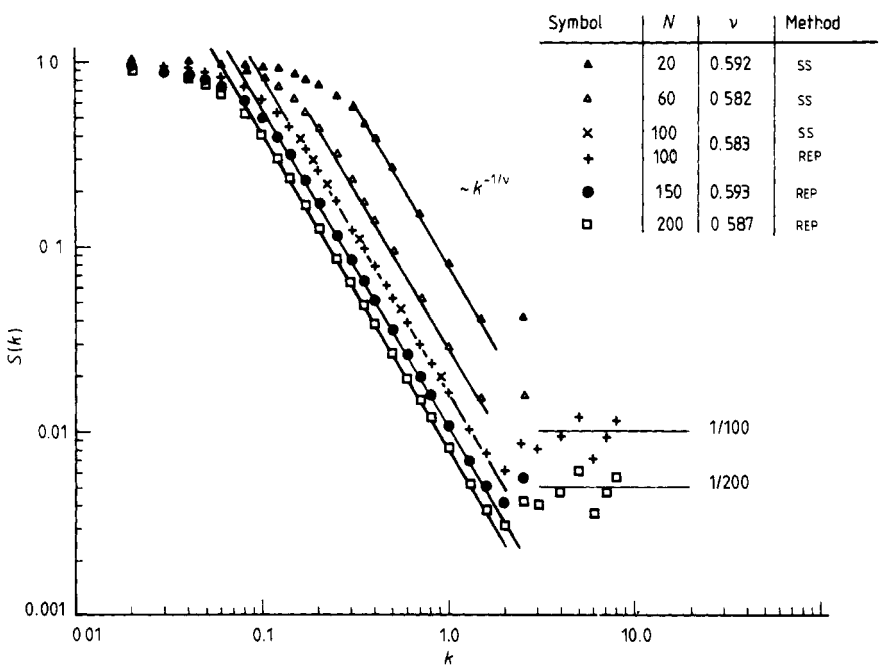

Figure 3. Log–log plot of $S(k)$ against k. Data from both simple sampling (SS) and reptation dynamics (REP) are shown.

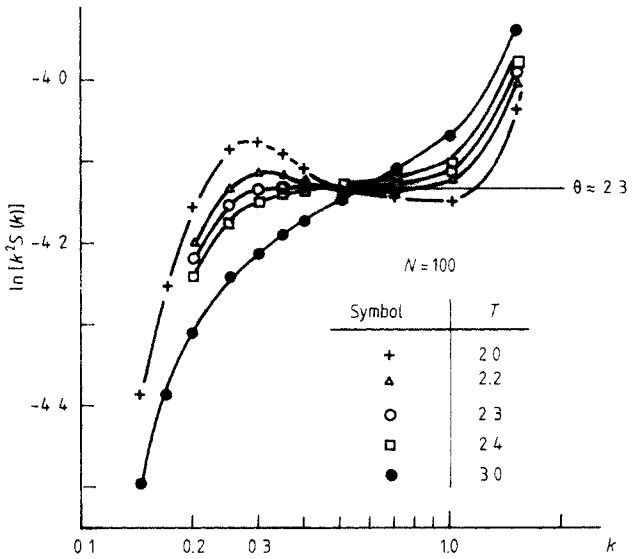

Figure 4. Log–log plot of $k^2S(k)$ against k for $N = 100$. Data are averaged over 250 000 chains generated by the SS method.

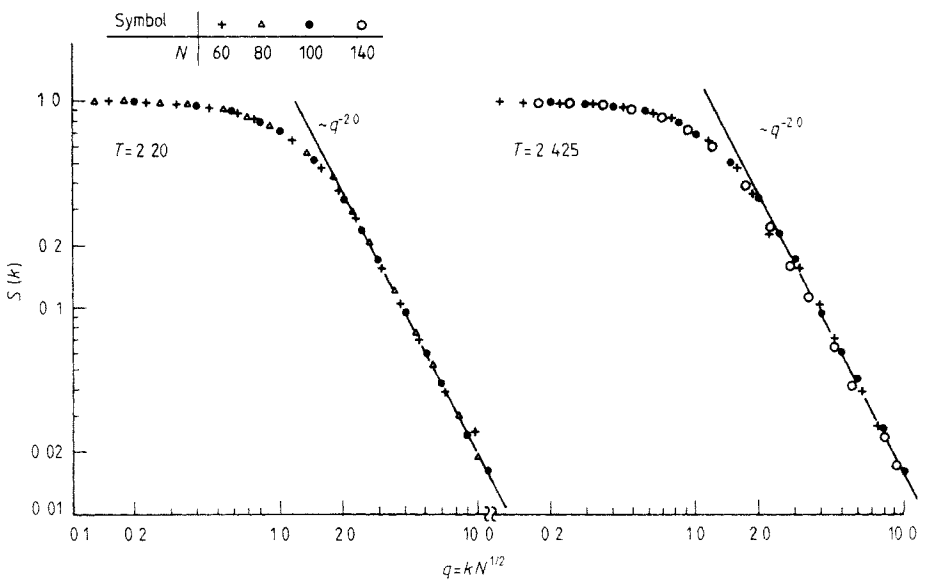

Figure 5. Log–log plot of $S(k)$ against scaling variable $q = kN^{\nu_t}$, $\nu_t = \frac{1}{2}$. Data for $N \leq 100$ are due to SS, data for $N = 140$ due to the reptation method.

Daoud and Jannink (1976). For $\langle R_N^2 \rangle$ the corresponding crossover scaling description reads

$$\langle R_N^2 \rangle^{1/2} \propto N^{\nu_t} f_{\pm}(N\tau^{1/\varphi_t}), \tag{15}$$

where the tricritical crossover exponent $\varphi_t = \frac{1}{2}$ (Fisher 1974), and the scaling functions

$f_{\pm}(x)$ must have the following behaviour:

$$f_+(x) = \begin{matrix} x^{\nu-\nu_t} & x \to \infty \\ \text{constant} & x \to 0 \end{matrix}, \qquad T > \theta, \tag{16a}$$

$$f_-(x) = \begin{matrix} x^{1/3-\nu_t} & x \to \infty \\ \text{constant} & x \to 0 \end{matrix}, \qquad T < \theta. \tag{16b}$$

We have checked equation (16*a*) only, since the ss data for $T < \theta$ and large N have rather large statistical uncertainties. From figure 6(*a*) rather distinct and systematic deviations from the expected scaling form are apparent. But one must note that equation (15) should hold only asymptotically in the limit $\tau \to 0$, $N \to \infty$, $N\tau^{1/\varphi_t}$ finite, while at not so small values of τ and $1/N$ there are correction terms to the asymptotic form. In fact, the variable τ in figure 6 becomes as large as about 0.3; hence part of the correction terms can be accounted for if we allow for a more general dependence on τ than just by the factor $\tau^{1/\varphi_t} = \tau^2$. This fact is illustrated in figure 6(*b*), where the τ dependence is assumed of a similar form, $\tau^{1/\varphi_{\text{eff}}}$, but φ_{eff} is chosen to fit the data reasonably well to a single curve, which occurs for $\varphi_{\text{eff}} = 2.5$ for data in the present temperature regime. Of course, in principle, φ_{eff} must thus depend on the range of temperatures to be fitted, and $\varphi_{\text{eff}}(\tau) \to \varphi_t = \frac{1}{2}$ as $\tau \to 0$. Since on short length scales there is clearly some stiffness of the chains at all temperatures, corrections due to the finiteness of N also occur, and hence one must expect still some systematic errors in the scaling function f_+ apparent from figure 6(*b*). But both figures 6(*a*) and 6(*b*) suggest that in the limit $\tau \to 0$, $N \to \infty$, a scaling function with the expected behaviour, equation (16*a*), may indeed be appropriate. Since equations (15), (16) can be derived from a 'blob picture' (de Gennes 1978, 1979), our results imply that there is no contradiction with the latter. Curro and Schäfer (1980) have reached a different

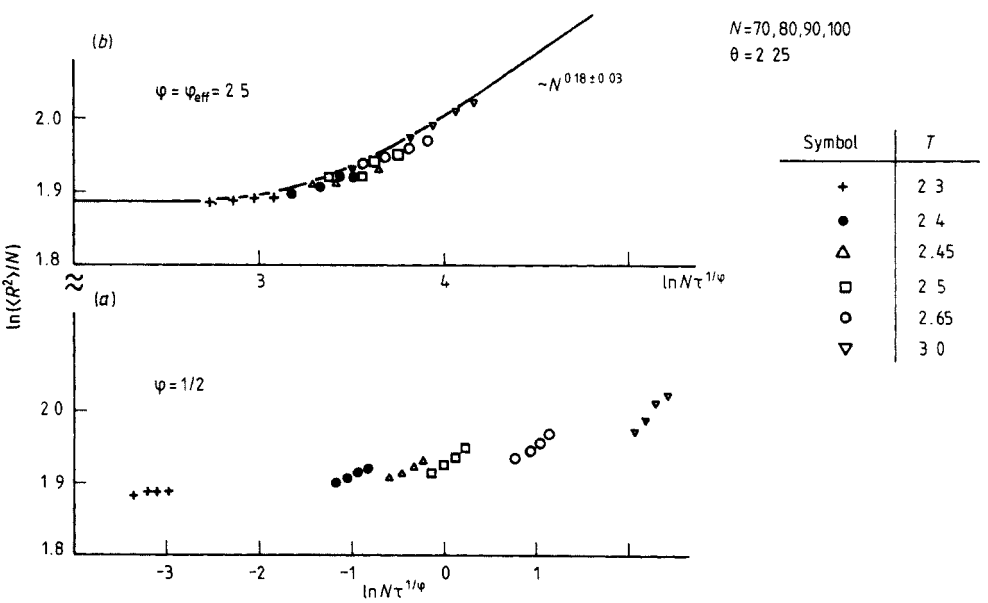

Figure 6. Log-log plot of the expansion factor $\langle R^2 \rangle / N$ against the scaling variable $N\tau^{1/\varphi}$ with (*a*) $\varphi = 1/2$ and (*b*) $\varphi_{\text{eff}} = 2.5$ for $\theta = 2.25$.

conclusion from data similar to those shown in figure 2; we feel that their data also reflect the stiffness of the chains at short distances, and do not exclude an interpretation such as done here in figure 6. In fact, for the related problem of crossover between self-avoiding walks and unrestricted random walks in the continuum (Kremer *et al* 1981), there is no stiffness of chains at short distances, and the expected scaling behaviour, equation (15), has been seen rather clearly. In this case one also has good agreement with the expected theoretical exponent $\varphi_t = \frac{1}{2}$.

A similar analysis applies to the structure factor as well, which must depend on the two scaled variables $N^{\nu_t}k$, $N\tau^{1/\varphi_t}$:

$$S(k) \propto (N^{\nu_t}k)^{-1/\nu_t} h_{\pm}(N\tau^{1/\varphi_t}, kN^{\nu_t}). \tag{17}$$

Since equation (14a) implies that for $kN^{\nu_t} \gg 1$ the only N-dependence of $S(k)$ is given by the $(1/N)$ prefactor, $h_{\pm}(x, y)$ must be a function of xy^{-1/ν_t} only for large N,

$$S(k) \propto (Nk^{1/\nu_t})^{-1} h_{\pm}(\tau^{1/\varphi_t} k^{-1/\nu_t}). \tag{18}$$

The scaling function $h_{\pm}$ behaves as

$$h_{\pm}(z) = \begin{cases} \text{constant}, & z \to 0, \\ z^{-1+\nu_t/\nu}, & z \to \infty, \end{cases} \tag{19}$$

where $\nu = 0.59$ for $T > \theta$, and hence $h_+(z \to \infty) \propto z^{-0.15}$, while $\nu = \frac{1}{3}$ for $T < \theta$, and hence $h_-(z \to \infty) \propto z^{1/2}$.

This behaviour, of course, can be derived by directly appealing to the 'blob picture' of de Gennes (1978, 1979). There the chain is thought to consist of 'blobs', i.e. subchains, containing $N_b \propto \tau^{-1/\varphi_t}$ units, each of which basically behaves like an ideal random walk. Hence, one should have, from equation (14a), using $\langle R^2_{N_B} \rangle \propto l^2 N_B$,

$$NS(k) \propto k^{-1/\nu_t}, \qquad l^2/(2\pi)^2 \ll k^{-2} \ll l^2 N_b/(2\pi)^2, \tag{20a}$$

while

$$NS(k) \propto k^{-1/\nu}, \qquad l^2 N_B/(2\pi)^2 \ll k^{-2} \ll \langle R^2_N \rangle/(2\pi)^2. \tag{20b}$$

Measuring lengths in such units that $(l/2\pi)^2 \equiv 1$, the ideal behaviour, equation (20a), is observed for the following regime of the scaling variable $y = kN^{\nu_t}$:

$$N_B^{-2\nu_t} \ll (kN_B^{\nu_t})^{-2} \ll 1, \qquad \text{or } \tau^{2\nu_t/\varphi_t} \ll (k^{1/\nu_t}\tau^{1/\varphi_t})^{2\nu_t} \ll 1, \tag{21a}$$

while the non-ideal behaviour, equation (20b), is observed for (remember $\langle R^2_N \rangle^{1/2} \propto N_B^{\nu_t}(N/N_B)^{\nu}$)

$$1 \ll (kN_B^{\nu_t})^{-2} \ll (N/N_B)^{2\nu}, \qquad \text{or } 1 \ll (k^{-1/\nu_t}\tau^{1/\varphi_t})^{2\nu_t} \ll N^{2\nu}\tau^{\nu/\varphi_t}. \tag{21b}$$

Therefore the crossover from ideal behaviour in the θ-regime to non-ideal behaviour occurs when the scaling variable $z = \tau^{1/\varphi_t} k^{-1/\nu_t}$ becomes large, in agreement with equations (18), (19).

Figure 7(a) shows the corresponding scaling plots for both $T > \theta$ and $T < \theta$. Once again systematic deviations from scaling behaviour are apparent, but become less pronounced if we use an effective φ, similar to above, instead of $\varphi_t = \frac{1}{2}$ expected for $\tau \to 0$. The resulting scaling functions (figure 7(b)) show rather well the behaviour concluded from equation (19); although the scaling functions as estimated in figure 7 may again be somewhat inaccurate, as some systematic errors due to use of too large values of variables τ, $1/N$, and k may still be present, qualitative consistency with the blob picture is demonstrated.

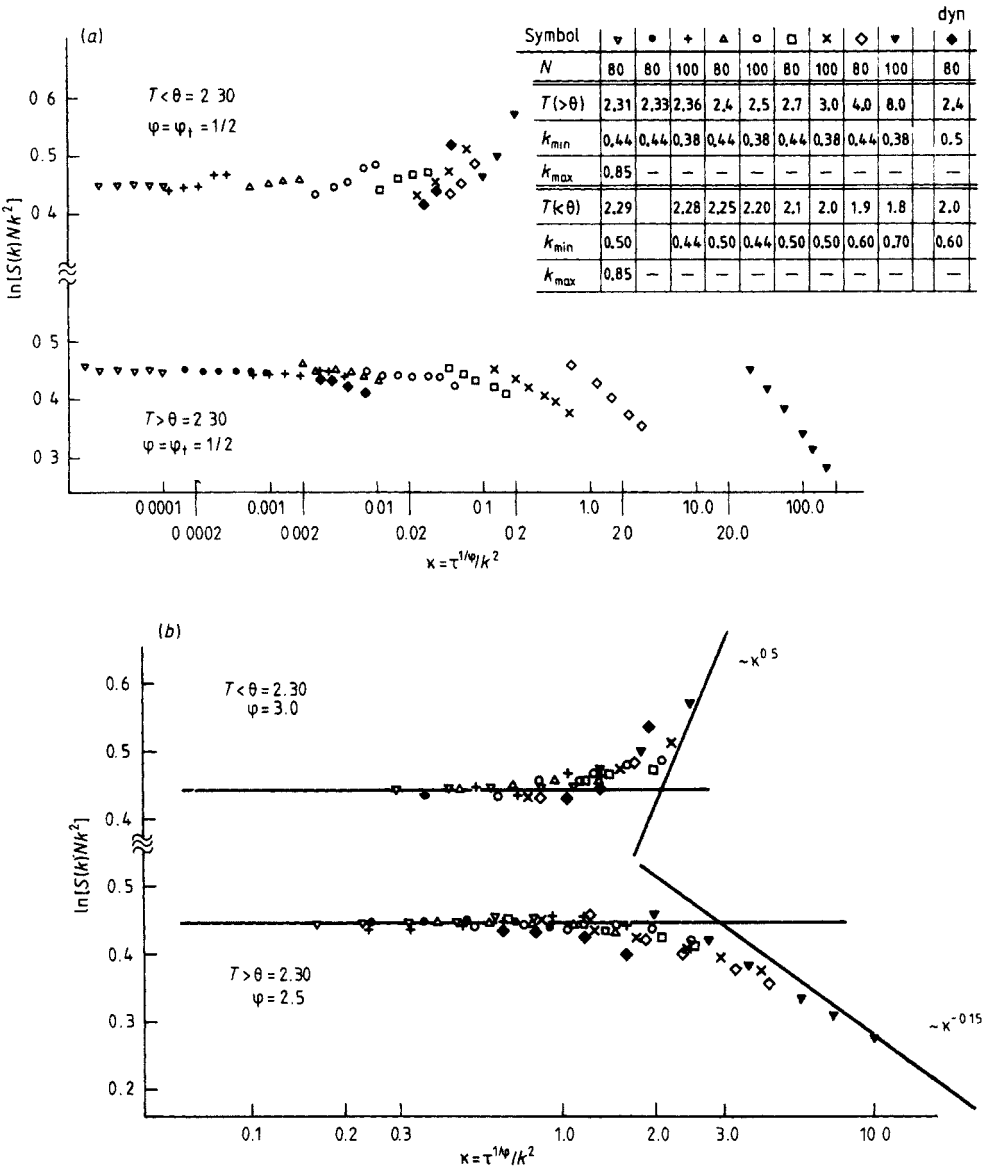

Figure 7. Scaling plot of the normalised structure factor $Nk^2S(k)$ against $k^{-2}\tau^{1/\varphi}$ for (*a*) $\varphi = \frac{1}{2}$ and (*b*) $\varphi_{\text{eff}} = 3$ ($T > \theta$) or $\varphi_{\text{eff}} = 2.5$ ($T < \theta$), respectively. Here $\theta = 2.3$ was chosen; chain lengths and temperatures used are indicated in the figure.

4.3. Free energy, entropy and specific heat

Next the free energy of the chain as well as its temperature derivatives are examined. While in dynamic simulations energy and specific heat are obtained in a straightforward manner (Binder 1979), it is more difficult to obtain the free energy itself. For example, one may estimate free energy differences from 'thermodynamic integration' (e.g. Binder 1981). From ss methods one obtains both free energy and entropy directly.

Since we are mainly interested in the free energy difference ΔF between SAWs and NRRWs, for which the entropy is known exactly, we have

$$\frac{-\Delta F(N,T)}{k_B T} = \frac{1}{k_B T}[F_{\mathrm{NRRW}}(T=\infty, N) - F_{\mathrm{SAW}}(T,N)] = \ln\left(\frac{Z_{\mathrm{SAW}}(T,N)}{Z_{\mathrm{NRRW}}(T=\infty,N)}\right) \quad (22a)$$

where $Z_{\mathrm{SAW}}(T,N)$ is the partition function of the generated SAWs, and Z_{NRRW} the partition function of NRRWs. Constructing NRRWs by the SS method, every attempt to generate a chain is successful. The ratio $Z_{\mathrm{SAW}}(T=\infty,N)/Z_{\mathrm{NRRW}}(T=\infty,N)$ is hence estimated from the fraction of successful SAWs constructions; denoting the fraction of walks with n nearest-neighbour contacts by $P_N(n)$, we then have

$$Z_{\mathrm{SAW}}(T,N)/Z_{\mathrm{NRRW}}(T=\infty,N) = \sum_n P_N(n)\exp(n\varepsilon/k_B T). \quad (22b)$$

In figure 8 it is seen that the resulting free energy difference is nearly independent of N in the θ-region. Following des Cloizeaux (1976) for $N\to\infty$, the free energy can be written as

$$F_{\mathrm{SAW}}(T,N)/k_B T = -N\ln q_{\mathrm{eff}}(T) - (\gamma-1)\ln N \quad (23)$$

where $q_{\mathrm{eff}}(T)$ can be interpreted as effective coordination number of the chain. Since

$$F_{\mathrm{NRRW}}(T,N)/k_B T = -N\ln(q-1), \qquad q=4, \quad (24)$$

the independence of N in the θ-region implies already that $q_{\mathrm{eff}}(T\approx\theta) = q-1$ and $\gamma = \gamma_t = 1$ in equation (23), while for T outside the θ-region $\gamma \approx \frac{7}{6}$(de Gennes 1979).

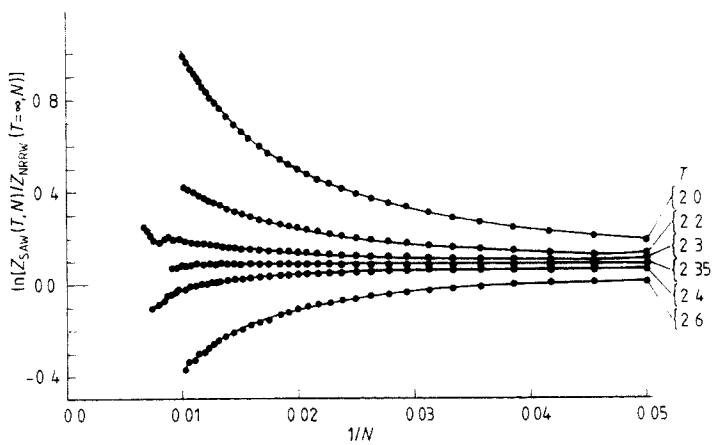

Figure 8. Simple-sampling data (with 2×10^6 samples for $N=100$) for the free energy difference $\Delta F/k_B T$ defined in equation (22).

In order to extract γ from the data, we consider the free energy difference, using equation (23),

$$\frac{\Delta F_N}{k_B T} \equiv [\Delta F(N+2,T) - \Delta F(N,T)] = 2\left[\ln\left(\frac{q-1}{q_{\mathrm{eff}}}\right) - \frac{\gamma-1}{N} + \mathrm{O}\left(\frac{1}{N}\right)^2\right]. \quad (25)$$

In equation (25) it is important to use $\Delta N = 2$ instead of $\Delta N = 1$, to get rid of the typical odd–even oscillations which otherwise occur in non-uniform lattices. For

reducing statistical scatter, we furthermore apply a 'triangle smoothing'

$$(\Delta F_N/k_BT)_{\text{smoothed}} = (14k_BT)^{-1}[8\Delta F_N + 2(\Delta F_{N+1} + \Delta F_{N-1}) + \Delta F_{N-2} + \Delta F_{N+2}]. \quad (26)$$

Plotting these data in figure 9 against $2/N$, the slope of the straight line yields $(\gamma - 1)$. As expected, the effective exponent deduced in this way is $\gamma_{\text{eff}} \approx 1$ throughout the θ-region.

Figure 10 shows an analogous plot for the entropy differences ($E(N, T)$ is the internal energy of a chain)

$$\Delta S_N/k_BT = [E(N, T) - E(N+2, T) - \Delta F(N+2, T)]/k_BT. \quad (27)$$

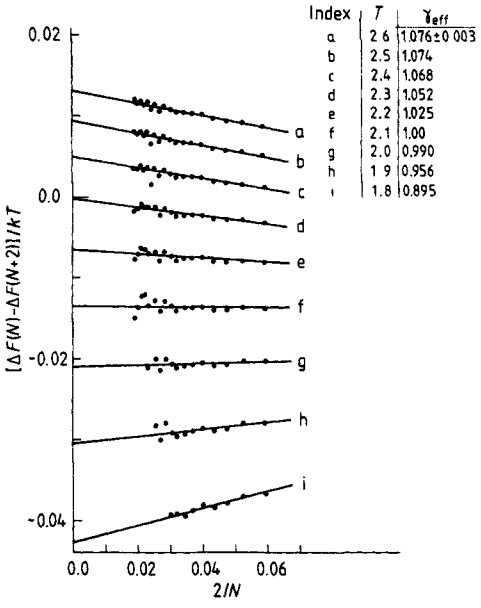

Figure 9. Plot of $\Delta F_N/k_BT$ against $2/N$ for various temperatures. The 'effective exponents' γ_{eff} deduced from the slopes are also shown.

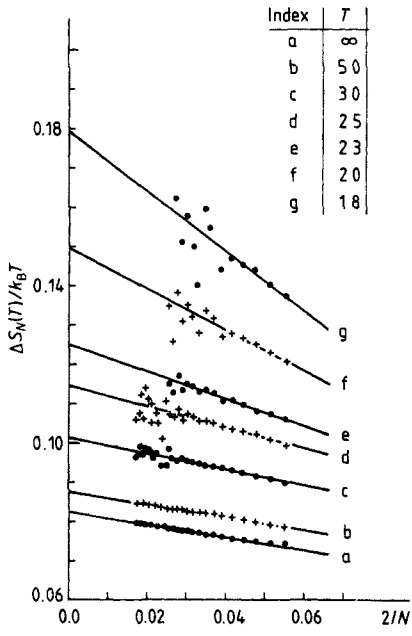

Figure 10. Plot of $\Delta S_N/k_BT$, defined in equation (27), against $2/N$ for various temperatures.

Since the entropy should behave similarly to the free energy, equation (23),

$$S_{\text{SAW}}(T, N)/k_BT = -N \ln s_{\text{eff}}(T) - (\gamma - 1) \ln N, \quad (28)$$

one should be able to deduce γ as well from ΔS_N, equation (28), by a formula analogous to equation (25)

$$\Delta S_N/k_BT = 2\{\ln[(q-1)/s_{\text{eff}}(T)] - (\gamma - 1)/N\}, \qquad N \to \infty. \quad (29)$$

For $T \gg \theta$, the data indeed are nicely consistent with the expected exponent $\gamma = \frac{7}{6} \approx 1.167$, and $s_{\text{eff}}(T = \infty) \equiv q_{\text{eff}}(T = \infty) = 2.880 \pm 0.002$, in excellent agreement with earlier investigations of this lattice (Watts 1975). But as T is lowered, one finds that γ_{eff} in this plot is monotonously increasing, and no evidence for $\gamma_{\text{eff}} \approx 1$ in the θ-region is seen. We feel, however, that the behaviour seen in figure 10 is due to the rapid variation of $s_{\text{eff}}(T)$ as one crosses the θ-region: for $T \to 0$, the chain configurations are some sort of 'Hamilton walks' (Gujrati 1980), with 'holes' whose concentration

is of order $\exp(-l\varepsilon/k_BT)$, where l is the number of bonds by which the energy is changed relative to its ground state value by each of these defects. Clearly, the entropy in the collapsed state well below θ will be much smaller than above θ, while the free energy is much less rapidly varying: the loss in entropy is largely compensated for by the gain in internal energy when entering the collapsed region. While $s_{\text{eff}}(T<\theta)$ is hence rather small, one still observes a fairly large entropy for short chains, because there is much entropy left due to the surface configurations of a short chain forming a collapsed coil. As a consequence, one has to proceed to very large N to see the asymptotic behaviour where equations (28), (29) are valid.

We now turn to the specific heat. Since renormalisation group arguments imply for very large chains near the θ-temperature (de Gennes 1978, Duplantier 1980)

$$F(N,T)/k_BT \propto N\tau^2|\ln|\tau||^p, \qquad p=\tfrac{3}{11}, \tag{30}$$

one expects an (albeit very weak) singularity in the specific heat, which is the second derivative of F with respect to temperature, and can be obtained from both ss and 'dynamic' Monte Carlo methods by considering energy fluctuations

$$\frac{C(T,N)}{\varepsilon N}=\frac{1}{N}\frac{\partial}{\partial T}\frac{E(T,N)}{\varepsilon}=\frac{1}{NT^2}(\langle E^2\rangle-\langle E\rangle^2) \tag{31a}$$

or

$$C(T,N)/\varepsilon N=(1/NT^2)(t_f-t_i)^{-1}\int_{t_i}^{t_f}\mathrm{d}t(E(t)-\langle E\rangle)^2. \tag{31b}$$

Figure 11 shows that the specific heat peak occurs at temperatures T distinctly below θ for the chain lengths available, and C is completely flat and monotonously decreasing at temperatures near θ. As N increases, the position θ_c of the maximum moves rather regularly towards θ (see figure 13 below), but the behaviour of $C_{\max}$ with N is rather irregular. This already occurs for very small N, where exact enumerations (Kennedy 1978) are available, and hence we feel that the irregular behaviour for larger N is a systematic effect, and not only due to the statistical inaccuracy of our data. To establish the asymptotic behaviour $C_{\max}/N\varepsilon \propto |\ln|N||^p$, which is expected from equation (28) assuming that the divergence of C is rounded off for scaling variables $N\tau^2$ of order unity, one clearly would have to study much larger N. Thus we cannot distinguish equation (28) from the somewhat different prediction $p=1$ due to Moore (1977). The unimportance of the logarithmic term in the free energy, for the regions of N,τ available to us, is also a justification to neglect logarithmic corrections in our crossover scaling analysis of the data on $S(k)$ and $\langle R_N^2\rangle$.

Another argument to show that very large N are required before one can expect to see the asymptotic behaviour of $C(N,T)$ is due to a consideration of the probability distribution $P_N(n)$ to have n nearest-neighbour contacts in a SAW of length N, since due to equation (22) C is closely related to that function. Now figure 12 shows that the structure of $P_N(n)$ is qualitatively different for small N and for large N: $P_N(n)$ decreases monotonically with n for small N, while for larger N ($N\sim 70$) a well defined maximum develops.

Nevertheless the specific heat is valuable to establish how the width of the θ-region varies with N. Figure 13 shows that the position θ_c of the specific heat maximum varies very regularly with N, in contrast to the height $C_{\max}$ itself, and satisfies a relation $(\theta-\theta_c)\propto N^{-1/2}$. Since the density increases rapidly at θ_c (figure 11(*b*)), θ_c is some

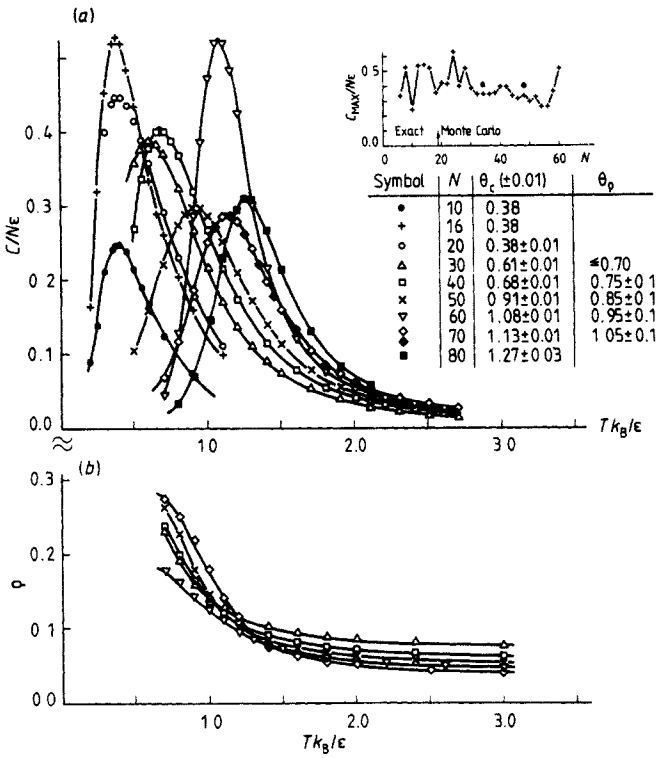

Figure 11. (*a*) Specific heat plotted against temperature for several chain lengths N. For $N<20$ exact enumerations were used (Kennedy 1978), other data are based on the SS method, using equation (29*a*). For $N=70$ also the differentiation was performed (full symbols). θ_c denotes the position of the specific heat maximum, the height C_{max} of this maximum being given in the insert. The dots there are based on dynamic Monte Carlo simulations using the reptation method and equation (29*b*). (*b*) Density ρ plotted against temperatures for various N. Temperature of maximal slope, θ_ρ, is given in (*a*).

effective smeared-out collapse transition temperature for finite chains. The temperature θ_c' where the free energy of a chain equals that of a NRRW also varies linearly with $1/\sqrt{N}$, and although for the range of N-values accessible here the estimates for θ are very different from each other, the two methods of defining an effective θ-temperature coincide nicely in the limit $N\to\infty$, and yield $\theta\approx 2.25$, in satisfying agreement with our analysis of $\langle R_N^2\rangle$ and $S(k)$.

The difference $\theta_c'-\theta_c$ in figure 13 must be of the same order of magnitude as the width $\Delta\theta$ of the θ-region, in which quasi-ideal behaviour of chains is observed, and hence figure 13 implies

$$\Delta\theta \propto N^{-1/2}. \tag{32}$$

This result is again in excellent agreement with the blob picture (de Gennes 1978) and renormalisation group arguments (Duplantier 1980), apart from logarithmic correction factors. The behaviour found here also agrees with recent experiments (Perzynski *et al* 1982).

In figure 13 we have also included the line of critical points $T_c(N)$ obtained from Flory–Huggins theory (Flory 1967), which extrapolates to $\theta_{\text{Flory–Huggins}}=2$, and the

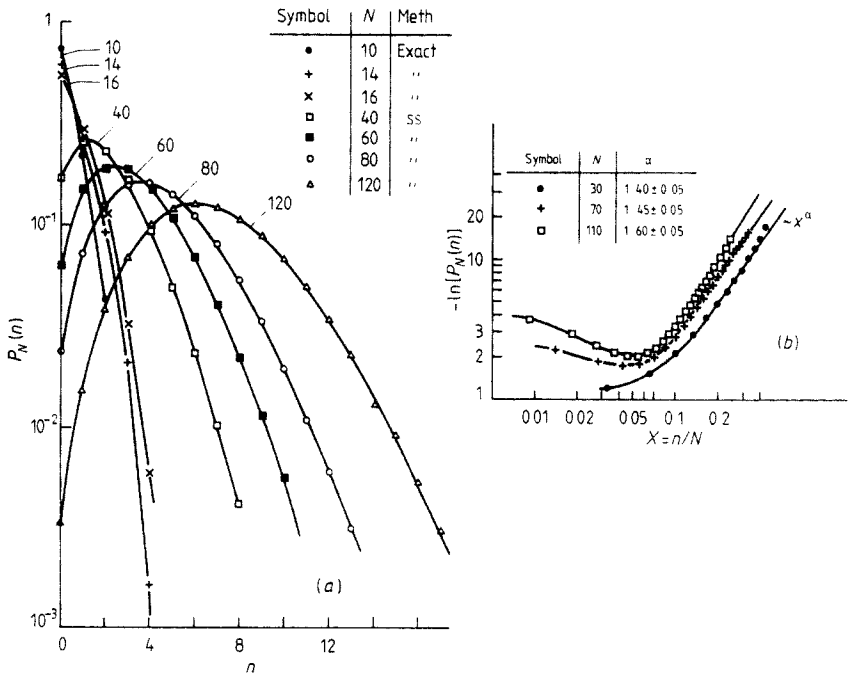

Figure 12. (*a*) Normalised distribution $P_N(n)$ (with $\Sigma_n P_N(n) = 1$) plotted against number n of nearest-neighbour contacts, for SAW at $T = \infty$ (see equation (22*b*)). (*b*) Log–log plot of $P_N(n)$ against the fraction x of contacts, to show the formula $P_N(n) \propto \exp(-x^{\alpha}$ constant) expected to hold for large enough x (Baumgärtner 1982). Preliminary estimates for the exponent α are included.

line of 'Boyle temperatures' $\theta_B(N)$ where the second virial coefficient $b(N, T)$ vanishes. Following Baumgärtner (1980) we compute a virial coefficient in terms of an average over simple random walks $\langle\ \rangle_0$,

$$b(N, T) = (N+1)^{-2} \sum_{\substack{i,j=1 \\ j>i}}^{N} \langle [\exp(-U_{ij}/kT) - 1] \rangle_0, \tag{33}$$

where $U = \infty$ if the SAW condition is violated, while otherwise $U_{ij} = \varepsilon$ for a nearest-neighbour contact. As expected, for instance, from renormalisation group arguments (de Gennes 1978), the limiting value of $\theta_B(N \to \infty)$, which may be interpreted as an 'unrenormalised' θ-temperature, is different from the actual θ-temperature. The same conclusion was also reached by Finsy *et al* (1975) for a virial coefficient defined from two-chain contacts (Janssens and Bellemans 1976, McKenzie and Domb 1967).

Finally we return to the behaviour of the density at low enough temperatures where our chain lengths suffice to study not only the θ-region but also the collapsed region. At these temperatures, neither SS nor reptation methods suffice, but the three–four bond motion technique still gives satisfactory results. Figure 14 shows that the density first decreases (these chain lengths correspond to chains still within the θ-region), then reaches a minimum and afterwards increases again. If one assumes a separation of the density in bulk and surface terms, $\rho(N, T) \approx \rho(\infty, T) - \rho_s(T) N^{-1/3}$, to hold in this region of N already, one would obtain an estimate for the bulk density

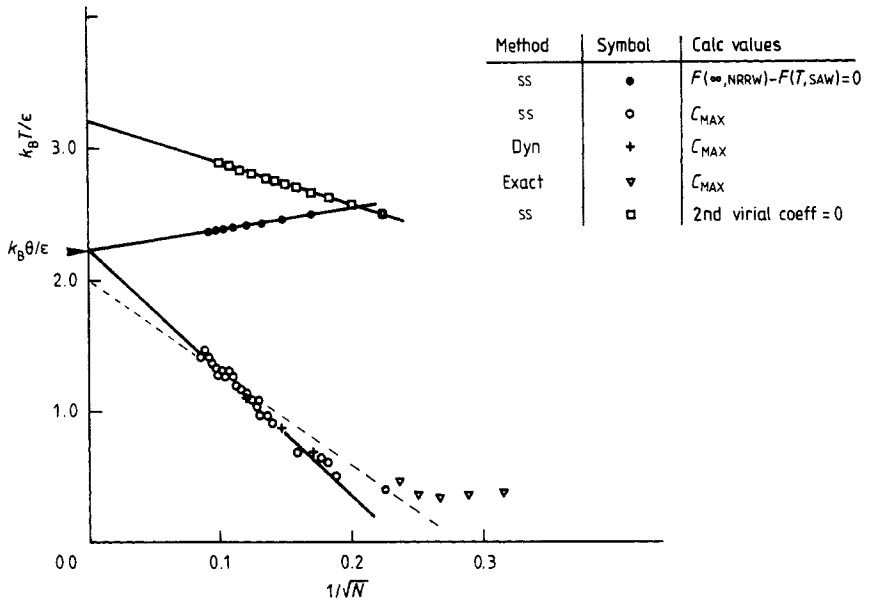

Figure 13. Various estimates for 'effective' θ-temperatures for chains of finite length plotted against $1/\sqrt{N}$. The lowest curve is composed of data of various methods; the 'dynamic' method is reptation for the two shorter chains, and three–four bond motion for the longer one. The dotted line gives the results for the Flory–Huggins theory. For further explanations cf text.

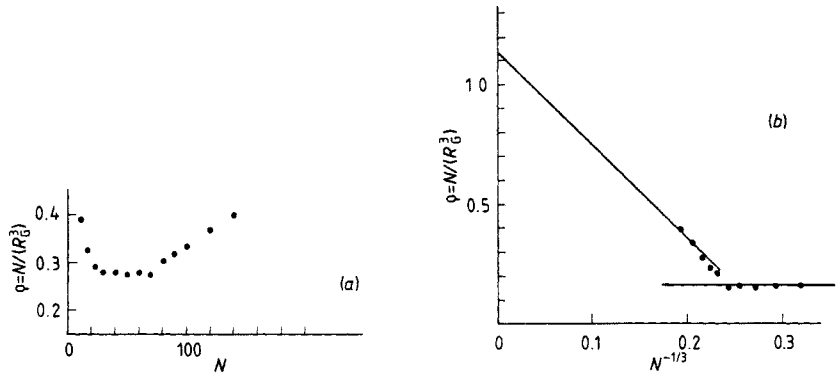

Figure 14. (*a*) Density ρ plotted against chain length N at $T = 1.1$. All data are due to dynamic three–four bond motion simulations, averaging over $5 \times 10^4 N^2$ attempted motions per chain. (*b*) Extrapolation of density against $N^{-1/3}$, to the expected ground state density $\rho_\infty \approx 1.13$ (Kremer 1982), for the same data as in (*a*).

$\rho(\infty, T)$ indistinguishable from the ground-state density $\rho(\infty, 0)$, which is readily estimated for any 'Hamilton walk' (Kremer 1982). Since the temperature shown in figure 14 is about $\frac{1}{2}\theta$, the decrease of density from its saturation value may indeed be very small. Unfortunately, our data are insufficient to examine the behaviour of $\rho(\infty, T)$ for T close to θ: one would need N much larger than $N_{\max}(T)$, where $N_{\max}(T)$ is the value of N for which the specific-heat maximum occurs at $\theta_c = T$ (figure 13),

in order to enter the collapsed region. Figure 14 also illustrates that estimating $\rho(\infty, T)$ from a region where the ρ against N curve is flat would be extremely misleading: for $N \approx N_{max}(T)$ a minimum in the ρ against N curve is reached, which should not be mistaken for an approach towards the bulk density of the collapsed coil.

5. Conclusions

This paper contains a rather extensive study of the behaviour of linear polymer chains on diamond lattices in the region around the θ-point, which we finally estimate as $\theta k_B/\varepsilon = 2.25 \pm 0.05$, for an energy $-\varepsilon$ of nearest-neighbour contacts on the lattice, and no other interactions (apart from the SAW restriction). This model on the one hand incorporates some of the steric effects occurring in real polymer chains such as alkanes, and on the other hand is simple enough to allow efficient Monte Carlo methods to be employed. Our numerical results agree with previous work on this lattice, as far as previous investigations went, and also are in qualitative agreement with previous studies for the θ-region of other models. But in our study, for the first time, data sufficient for a detailed comparison with crossover scaling concepts such as the blob picture have been obtained. Using effective crossover exponents to account for corrections to scaling, rough estimates for the crossover scaling function of the end-to-end distance and the structure factor were obtained. While the chains exhibit considerable stiffness on short length scales, one finds $\langle R_N^2 \rangle \propto \langle S_N^2 \rangle \propto N$ for $T = \theta$ for large N, and hence the prefactor of this relation is very different from a simple random walk on this lattice. Similarly, the temperatures where the second virial coefficient vanishes do not extrapolate towards the θ-temperature. At the θ-point, only the long-range SAW interactions and the attractive interactions cancel, but the short-range SAW condition, i.e. the NRRW condition, is not cancelled. This is consistent, of course, with observing stiffness on short length scales, and with the finding that for $T \to \theta$ the free energy becomes identical to that of NRRWs.

We have also estimated the width of the θ-region and found that it vanishes with an $N^{-1/2}$ law as $N \to \infty$, consistent with recent theoretical predictions and experiment. In the regime $T < \theta$, we predict a non-monotonic approach of the density towards its bulk value. It would be interesting if corresponding experiments on real alkane chains could be performed to see this behaviour also, as well as check our various other predictions.

Acknowledgment

The authors thank Dr J W Kennedy for informing us about the enumeration results.

References

Baumgärtner A 1980 *J. Chem. Phys.* **72** 871
—— 1981 *Polymer* **22** 1308
—— 1982 to be published
Baumgärtner A and Binder K 1979 *J. Chem. Phys.* **71** 2541
Binder K (ed) 1979 *Monte Carlo Methods in Statistical Physics* (Berlin: Springer)
—— 1981 *Z. Phys.* B**45** 61

Clark A T and Lal M 1977 *Br. Polym. J.* June 92
des Cloizeaux J 1976 *J. Physique* **37** 431
Cuniberti C and Bianchi U 1974 *Polymer* **15** 346
Curro J G and Schäfer D W 1980 *Macromolecules* **13** 1199
Daoud M and Jannink G 1976 *J. Physique* **37** 973
Debye P 1947 *J. Phys. Colloid Chem.* **51** 18
Domb C 1974 *Polymer* **15** 259
Domb C and Fisher M E 1958 *Camb. Phil. Soc.* **54** 48
Duplantier B 1980 *J. Physique Lett.* **41** L 409
Edwards S F 1965 *Proc. R. Soc.* A**85** 613
—— 1970 *J. Non-Cryst. Solids* **4** 417
Farnoux B, Boúe F, Cotton J P, Daoud M, Jannink G, Nierlich M and de Gennes P G 1978 *J. Physique* **39** 77
Finsy R, Janssens M and Bellemans A 1975 *J. Phys. A: Math. Gen.* **8** L106
Fisher M E 1974 *Rev. Mod. Phys.* **46** 597
Fisher M E and Hiley B J 1961 *J. Chem. Phys.* **34** 1253
Flory P J 1967 *Principles of Polymer Chemistry* (Ithaca, NY: Cornell University Press)
—— 1969 *Statistical Mechanics of Chain Molecules* (New York: Interscience)
de Gennes P G 1972 *Phys. Lett.* **38A** 339
—— 1975 *J. Physique Lett.* **36** 55
—— 1977 *Riv. Nuovo Cimento* **7** 363
—— 1978 *J. Physique Lett.* **39** 299
—— 1979 *Scaling Concepts in Polymer Physics* (Ithaca, NY: Cornell University Press)
Gény F and Monnerie L 1979 *J. Polym. Sci. Phys. Ed.* **17** 131, 147
Gujrati P D 1980 *J. Phys. A: Math. Gen.* **13** L 437
Hilhorst H J and Deutch J M 1975 *J. Chem. Phys.* **63** 5153
Janssens M and Bellemans A 1976 *Macromolecules* **9** 303
Kennedy J W 1978 *private communication*
Kirkpatrick S and Stoll E P 1981 *J. Comp. Phys.* **40** 517
Kremer K 1981 *Z. Phys.* B **45** 149
—— 1982 to be published
Kremer K, Baumgärtner A and Binder K 1981, *Z. Phys.* B **40** 331
Lal M and Spencer D 1971 *Mol. Phys.* **22** 649
Lax M and Brender C 1977 *J. Chem. Phys.* **67** 1785
Lifshitz J M, Grosberg A You and Khokklov A R 1978 *Rev. Mod. Phys.* **50** 683
McCrackin F L, Mazur J and Guttman C L 1973 *Macromolecules* **6** 859
McKenzie D S and Domb C 1967 *Proc. Phys. Soc.* **92** 632
Mazur J and McCrackin F L 1968 *J. Chem. Phys.* **49** 648
Mazur J and McIntyre D 1975 *Macromolecules* **8** 464
Moore M A 1977 *J. Phys. A: Math. Gen.* **10** 305
Nierlich M, Cotton J P and Farnoux B 1978 *J. Chem. Phys.* **64** 1379
Perzynski R, Adam M and Delsanti M 1982 *J. Physique* **43** 129
Rapaport D C 1974 *Phys. Lett.* **38A** 339
—— 1977 *J. Phys. A: Math. Gen.* **10** 637
Swislov G, Sun S T, Nishio J and Tanaka T 1980 *Phys. Rev. Lett.* **44** 796
Verdier P H 1966 *J. Chem. Phys.* **45** 2118, 2122
Wall F T and Hioe F T 1970 *J. Phys. Chem.* **74** 4410, 4416
Wall F T and Mandel F 1971 *J. Chem.* **63** 4592
Watts M G 1975 *J. Phys. A: Math. Gen.* **8** 61
Webman J, Lebowitz J L and Kalos M H 1980 *J. Physique* **41** 579
—— 1981 *Macromolecules* **14** 1495